DOI: 10.48011/sbse.v1i1.2395

Impedance-based Fault Location Error Analysis in Distribution Network with Distributed Generation ⋆

Guilherme Y. Kume * **Antonio E. C. Momesso** *
Felipe M. dos S. Monteiro * **Eduardo N. Asada** *

* *Department of Electrical and Computer Engineering, University of São Paulo, São Carlos, Brazil, (e-mail: {guilhermeyujikume, antonio.momesso, fmarkson, easada}@usp.br).*

Abstract: Reliability and continuity in the electrical system are one of the issues where distribution companies are continually seeking improvements. The penetration of Distributed Generators (DGs) contributes to modify the amplitude of the fault signals, which significantly affects the accuracy of the fault location algorithms. In this context, this paper proposes an impedance-based method to fault location in distribution systems with DGs. A new process analyzing the linear behavior of input and output information of the algorithm to search the short-circuits location is used. The smart meters were allocated at the substation and DGs nodes, and a real 135-bus distribution electrical system was used to perform the robustness tests. The results showed that the fault location method has high accuracy, and no significant influences on the location results regarding the penetration level have been observed. Because of its simplicity and high accuracy, we emphasize its applicability to realistic problems.

Keywords: Fault Location; Impedance-based Location; Distributed Generators; Distribution Systems.

1. INTRODUCTION

In power distribution systems, faults are the leading causes of supply interruption. The interruptions are responsible for the negative impacts system performance, such as damage to the distribution company's assets, financial losses, and continuity indices. Moreover, with the increasing penetration of Distributed Generators (DGs) in the distribution system, failures tend to be more severe and may cause further system damage. Therefore, distribution companies use fault location methods to mitigate these events and avoid further loss quickly (Perez et al., 2019).

Impedance-based fault location methods use steady-state voltage and current values to estimate the distance between the substation and the fault location. Due to their simplicity of calculation, these methods are widely used in distribution systems (Mora-Flòrez et al., 2008). Another reason for its use is due to the reduced availability of measurements and fault indicators installed in the distribution system. However, the impedance-based methods are affected by non-homogeneity of the distribution system, requiring additional approaches; multiple lateral branches, causing multiple location estimations; error in the line parameters, influencing the solution. However, if the system is homogeneous, with side branch fault indicators and no parameter errors, these methods have good accuracy (Gururajapathy et al., 2017).

⋆ This study was financed in part by the Coordenação de Aperfeiçoamento de Pessoal de Nível Superior – Brasil (CAPES) – Finance Code 001, and by the São Paulo Research Foundation (FAPESP) – grant 2018/23338-0

Among the works that propose the use of impedance-based methods, we highlight the papers that use three-phase components, because they can deal with the non-homogeneity of the distribution system. Jun Zhu et al. (1997) proposes a fault location scheme based on an interactive method that solves the equation that describes the steady-state fault condition. Using additional information from the protection and loading devices, a fault diagnostic algorithm is then used to determine the real fault location. In Ferreira et al. (2012) and Salim et al. (2009) is proposed a method that considers the particular characteristics of distribution systems as phase unbalance due to the presence of single-phase and two-phase branches, load profile variation, and the presence of line asymmetry. Dashti et al. (2018) proposes a fault location algorithm considering the fourth wire separately for four-wire networks using the π line model. The proposed fault location equations are second-order polynomials. Therefore, at each iteration of the algorithm, two fault distances are obtained, and only one solution is the real fault location. Thus, some conditions must be taken into consideration to determine the correct answer.

As can be seen, the papers presented do not consider the presence of DGs in the distribution system. Thus, in this context, the main contributions of this paper are: a study of the error behavior of the fault location by impedance method analyzing its variation concerning the distance of the fault occurrence, fault impedance and fault type; based on the error behavior, an iterative fault location method based on the impedance method is proposed. The proposed

method takes into consideration the contribution of DGs and loads in the distribution system.

This paper is organized as follows: This section presents an introduction to the problem and a brief review of the literature. In Section 2, the formulation of fault location problem and the solution technique is presented. Section 3 presents the numerical results of computer simulations of the proposed method with a real 135-bus distribution test system with three levels of DGs penetration. Finally, the conclusions and future work are presented in Section 4.

2. IMPEDANCE-BASED FAULT LOCATION METHOD

The proposed impedance method is divided into two sets of functions. The first is the local search; in other words, it is the search for the location of the short-circuit in a specific branch. The second is the global search, in which the search is performed in the system through the sections.

The first function is based on the analytical formulation based on Bahmanyar and Jamali (2017). For the short-circuit calculation, only resistive impedance is considered; in other words, the three-phase apparent power at the fault point is composed only by the real part, i.e., the reactive power (Q_F) is zero (1).

$$Q_F = Im\left(\mathbf{V_F}^T \cdot \mathbf{I_F}^*\right) = 0 \tag{1}$$

where $\mathbf{V_F}$ is the fault point voltage, and $\mathbf{I_F}$ is the short-circuit current.

The fault voltage can be written as a function of sending-end voltage ($\mathbf{V_S}$) and line parameters ($\mathbf{Z}$), as shown in (2).

$$\begin{bmatrix} V_{F_a} \\ V_{F_b} \\ V_{F_c} \end{bmatrix} = \begin{bmatrix} V_{S_a} \\ V_{S_b} \\ V_{S_c} \end{bmatrix} - d \cdot \begin{bmatrix} z_{aa} & z_{ab} & z_{ac} \\ z_{ba} & z_{bb} & z_{bc} \\ z_{ca} & z_{cb} & z_{cc} \end{bmatrix} \cdot \begin{bmatrix} I_{Sub_a} \\ I_{Sub_b} \\ I_{Sub_c} \end{bmatrix} \tag{2}$$

where $\mathbf{I_{Sub}}$ is the current vector of the substation contribution and d is the distance from the upstream fault bus and the short circuit point.

Fig. 1 shows a generic fault at point F, between two generic buses (S and R). The fault current is represented by $\mathbf{I_F}$, and the contribution of the DGs is given by $\mathbf{I_{DG}}$.

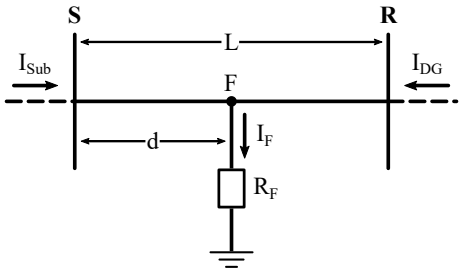

Figure 1. Generic fault in a branch.

Splitting the real and imaginary part of (2) and substituting on (1), the fault distance (d) can be written as a function of fault current (3). Besides, this equation does not depend on the fault type.

$$d = \frac{\sum\limits_{k=a,b,c} \left(V^r_{S_k} I^i_{F_k} - V^i_{S_k} I^r_{F_k}\right)}{\sum\limits_{j=a,b,c} \sum\limits_{l=a,b,c} \left[\left(R_{jl} I^r_{S_l} - X_{jl} I^i_{S_l}\right) I^i_{F_j} - \left(X_{jl} I^r_{S_l} + R_{jl} I^i_{S_l}\right) I^r_{F_j}\right]} \tag{3}$$

where k, j, and l are the three-phase system, r and i are real and imaginary parts of phasors.

2.1 Error analysis

Since the distance is an unknown variable and also is one of the input and output information of the algorithm, an investigation about the errors generated between the output and input are analyzed.

Based on the previous equations, with the following steps, the error among input and output distances can be calculated:

(i) Fault distance initialization: d_{in};
(ii) Fault point voltage determination: (2);
(iii) Downstream power flow resolution resulting in I_{DG};
(iv) Fault current calculation: $I_F = I_{Sub} + I_{DG}$;
(v) Fault distance estimation: d_{out} obtained by (3);
(vi) Error calculation: $error = d_{out} - d_{in}$.

The error behavior, according to the fault distance estimation, was analyzed for short-circuits in the first line section of the test system, presented in Section 3. For this, 100 points of the distance of initialization (d_{in}) were inserted, ranging 1% from the final line length. The distance (Fig. 2), impedance (Fig. 3), and type (Fig. 4) of fault were varied. The variation of the fault distance implied the line displacement (Fig. 2), while the change of the resistance and the type of fault led to the change in the inclination, as shown in Figs. 3 and 4. Also, for short-circuits near the substation, there is a strong correlation between the error and the estimated distance, reaching Pearson coefficient values higher than 0.99. On the other hand, for faults close to DGs, the correlation coefficient becomes less than -0.99. However, in both cases, the behavior can be approximated by a straight line equation.

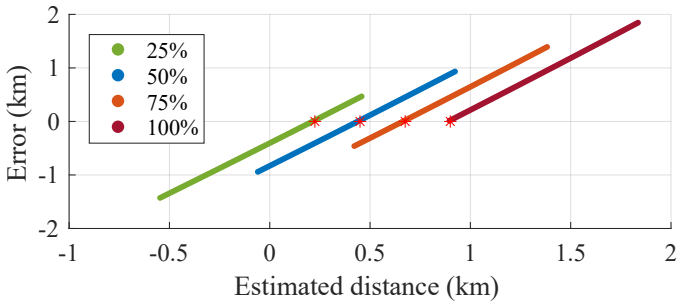

Figure 2. Estimated distance error as a function of fault distance variation in 25%, 50%, 75%, and 100% of line length.

2.2 Proposed method for algorithm convergence

From the observed characteristic of the errors, aiming to minimize the processing time, the fault distance was found through an iterative process (Fig. 5). For this, two points are chosen as inputs of the algorithm (d_{in1} and d_{in2}, given by start and end line distances), so the estimated distances

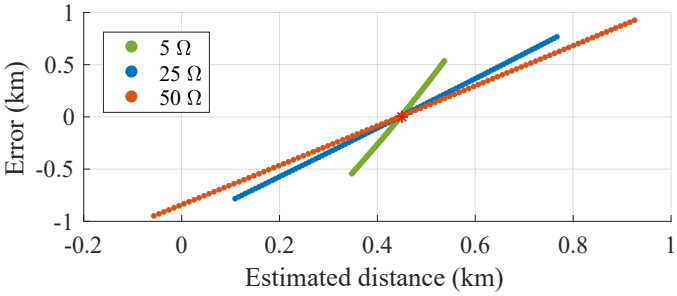

Figure 3. Estimated distance error as a function of fault resistance variation in 5 Ω, 25 Ω, and 50 Ω.

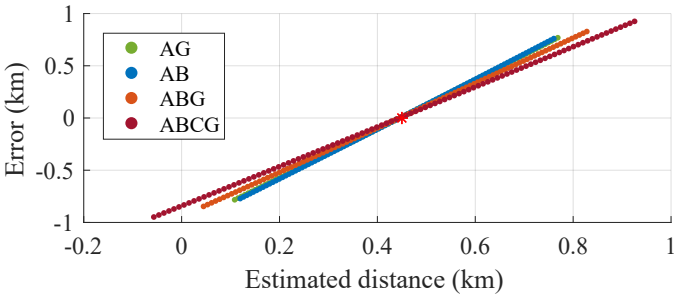

Figure 4. Estimated distance error as a function of fault type variation in single-phase, two-phase, two-phase to ground, and three-phase to ground.

(d_{out1} and d_{out2}) and errors are stored. With these points, the zero of the function is calculated from the equation of the straight line. Subsequently, the calculated distance becomes the input (d_{in3}), and a new distance is estimated (d_{out3}). The error is evaluated whether positive or negative. If positive, the function zero is recalculated with the distance which previous error is negative. Otherwise, the zero of the function is obtained with the distance which previous error is positive. The new estimated distance becomes the input, and the process is repeated until the tolerance is met. The distance which error is zero will result between the two points of the generated line. In this work, the tolerance for the convergence of the method was 0.1 m.

2.3 Global search of fault location

Although the algorithm so far describes a local search of the fault, the method searches the entire system. Initially, all system ends are identified. Later on, from the substation, where voltage and current measurements are available, the algorithm is executed. If in the first iteration, the estimated distance is greater than the line section length, then the next section will be analyzed, and the voltage drop equation updates the voltage based on the known branch impedance. Otherwise, the algorithm continues until the convergence. After selecting the next branch, the substation's contribution current is updated, and if any load is connected, its influence is removed. If a lateral branch is found, the current of this branch is calculated by the backward-forward sweep power flow and is discounted of I_{Sub}. The load model is constant power. However, if the voltage is less than a threshold, the model becomes constant impedance in order to help power flow converging, as presented in (4).

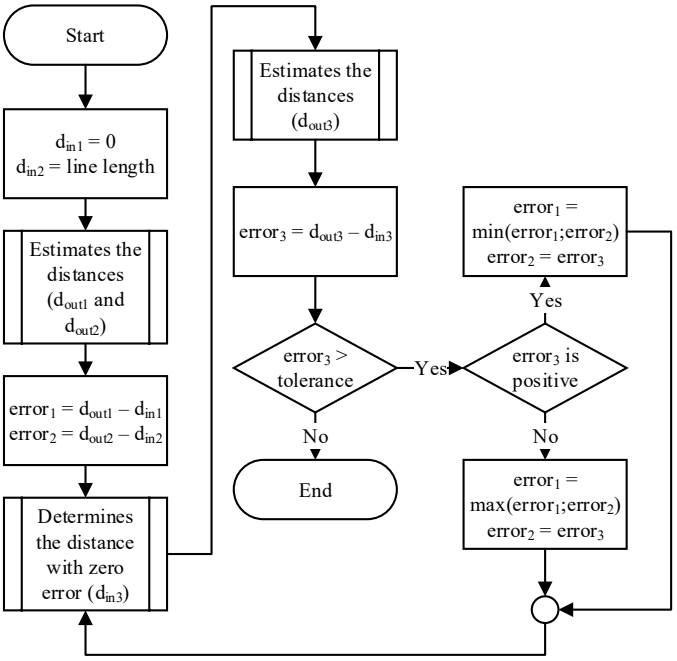

Figure 5. Flowchart of the proposed fault location method.

$$S = \begin{cases} S_0 \cdot \left(\frac{V_k}{V_0}\right)^n & for\ V_k \geq V_{min} \\ S_0 \cdot \left(\frac{V_{min}}{V_0}\right)^n \cdot \left(\frac{V_k}{V_{min}}\right)^2 & for\ V_k < V_{min} \end{cases} \quad (4)$$

where n is given by the load type: 0 for constant power; 1 for constant current; and 2 for constant impedance. V_k is the voltage applied to the load, V_{min} is the voltage limit to which the load changes characteristics, and S_0 and V_0 are the nominal load power and voltage, respectively.

As it is not possible to know at which branch the fault is occurring so that the line section can be located, it is necessary to analyze the entire feeder. Thus, the process runs to all system ends, and all possible fault locations are stored. In this situation, it is essential to reduce possible fault points so that maintenance personnel does not have to check every possible location. However, this paper will not address multiple location reductions, e.g., by allocating fault indicators (Farajollahi et al., 2019; Sau et al., 2020).

3. RESULTS

The studies were performed in a real 135-bus distribution test system (Fig. 6). The balanced loads totalize, approximately 6.5 MW and 2.77 MVAr, and were considered to be constant power for $V \geq 0.8$ pu. The equivalent impedance of the source was not considered. This feeder has an average length of 70 m, being the largest section with a length of 900 m and the smallest with 5 m. More information about the system can be found in (LaPSEE, 2019).

Three Synchronous Generators (SGs) were allocated on buses 88, 119, and 122. They have the power of 1.0 MW and 0.3 MVAr; 0.9 MW and 0.3 MVAr; and 0.3 MW and 0.1 MVAr, respectively. The transformer of connection (4.16 kV - 13.8 kV) has a nominal power of 1.5 MVA, copper losses of 0.7%, and leakage reactance of 6%. Also,

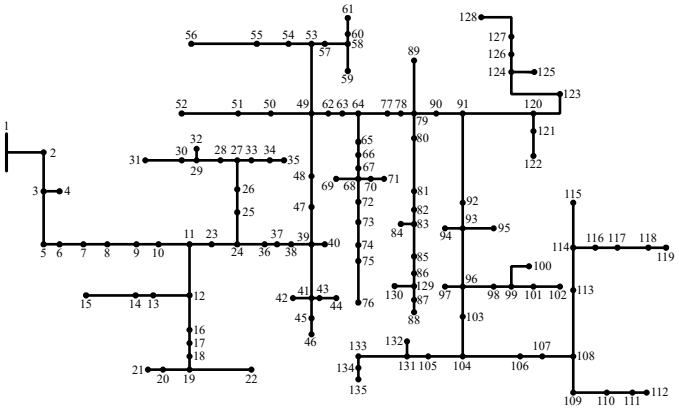

Figure 6. 135 bus system.

the SGs were adjusted to control the injected active and reactive power.

It was considered that there are measurements available at the substation and DGs. The data of the voltages and currents, during the fault, were obtained by the OpenDSS software. With this information, the distances were calculated using the equations presented in Section 2, with the C++ language. The power demand is known, and no measurement error has been considered in the calculations of the distances.

Simulation cases include variations on the penetration of DGs, the length of the line to which the short circuit was applied, the fault resistance, and the type. For each line section, the four cases have been simulated, totaling 19,296 faults. The algorithm performance was evaluated by error analysis given by the modulus of the difference between the actual and estimated distance, in meters, from the fault location to the substation. The results were grouped, and the mean (μ), standard deviation (σ), maximum, and minimum are presented.

3.1 One generator in the system

In this first case, the presence of a SG, connected to bus 119, was considered (farthest bus from the substation).

Table 1 shows the mean, standard deviation, maximum, and minimum errors for faults applied to 25% of the line section. For the four types of fault, the resistance was varied. For faults of 5 Ω, regardless of the type of fault, the mean of errors was close to zero. Also, the mean of errors increases as the fault resistance increases for all types, being higher in the case of single-phase faults with the resistance of 50 Ω. This case also presented the largest dispersion of error, reaching a maximum value of 0.130 m. The largest error, considering all cases, was for a three-phase to ground fault, with the resistance of 50 Ω (0.135 m), between buses 118 and 119, which section length is 70 m.

Table 2 shows errors for faults applied at 50% of the line section length. In general, the same average and standard deviation of Table 1 are found, varying, in some cases, only the minimum value. Again, the biggest error occurred for 50 Ω three-phase to ground fault between buses 118 and 119.

Table 1. Faults applied to 25% of line section length considering one generator

Error (m)	5 Ω	25 Ω	50 Ω	5 Ω	25 Ω	50 Ω
	AG			**AB**		
μ	0.001	0.016	0.070	0.000	0.007	0.026
σ	0.000	0.003	0.022	0.000	0.002	0.008
Maximum	0.001	0.021	0.130	0.001	0.011	0.050
Minimum	0.000	0.007	0.006	0.000	0.003	0.008
	ABG			**ABCG**		
μ	0.000	0.010	0.043	0.000	0.012	0.044
σ	0.000	0.003	0.014	0.000	0.004	0.020
Maximum	0.001	0.016	0.077	0.001	0.020	0.135
Minimum	0.000	0.003	0.012	0.000	0.004	0.002

Table 2. Faults applied to 50% of line section length considering one generator

Error (m)	5 Ω	25 Ω	50 Ω	5 Ω	25 Ω	50 Ω
	AG			**AB**		
μ	0.001	0.016	0.070	0.000	0.007	0.026
σ	0.000	0.003	0.022	0.000	0.002	0.008
Maximum	0.001	0.021	0.130	0.001	0.011	0.050
Minimum	0.000	0.005	0.006	0.000	0.003	0.008
	ABG			**ABCG**		
μ	0.000	0.010	0.043	0.000	0.012	0.044
σ	0.000	0.003	0.014	0.000	0.004	0.020
Maximum	0.001	0.016	0.077	0.001	0.020	0.135
Minimum	0.000	0.004	0.008	0.000	0.002	0.002

Tables 3 and 4 show the mean, standard deviation, maximum, and minimum errors for faults applied to 50% and 75% of the line section, respectively. Both tables have the same mean and standard deviation values, differing from Tables 1 and 2 in some cases. However, again, single-phase faults with a resistance of 50 Ω presented higher mean error, being also the largest found for a three-phase to ground fault with a resistance of 50 Ω.

Table 3. Faults applied to 75% of line section length considering one generator

Error (m)	5 Ω	25 Ω	50 Ω	5 Ω	25 Ω	50 Ω
	AG			**AB**		
μ	0.001	0.016	0.070	0.000	0.007	0.026
σ	0.000	0.003	0.022	0.000	0.002	0.008
Maximum	0.001	0.021	0.130	0.001	0.011	0.050
Minimum	0.000	0.008	0.006	0.000	0.003	0.008
	ABG			**ABCG**		
μ	0.001	0.010	0.043	0.000	0.012	0.045
σ	0.000	0.003	0.013	0.000	0.004	0.020
Maximum	0.001	0.016	0.077	0.001	0.020	0.135
Minimum	0.000	0.004	0.012	0.000	0.002	0.003

Table 4. Faults applied to 99% of line section length considering one generator

Error (m)	5 Ω	25 Ω	50 Ω	5 Ω	25 Ω	50 Ω
	AG			**AB**		
μ	0.001	0.016	0.070	0.000	0.007	0.026
σ	0.000	0.003	0.022	0.000	0.002	0.008
Maximum	0.001	0.021	0.130	0.001	0.011	0.050
Minimum	0.000	0.008	0.005	0.000	0.003	0.008
	ABG			**ABCG**		
μ	0.001	0.010	0.043	0.000	0.012	0.045
σ	0.000	0.003	0.013	0.000	0.004	0.020
Maximum	0.001	0.016	0.077	0.001	0.020	0.134
Minimum	0.000	0.004	0.012	0.000	0.004	0.002

3.2 Two generators in the system

In this case, in addition to the SG at bus 119, another generator, with a power of 1.0 MW and 0.3 MVAr, was connected to bus 88.

Comparing Tables 5 and 6 is possible to verify that both have the same values of mean error and standard deviation, differing only in the maximum error found when a single-phase fault occurs with a resistance of 50 Ω.

Table 5. Faults applied to 25% of line section length considering two generators

Error (m)	5 Ω	25 Ω	50 Ω	5 Ω	25 Ω	50 Ω
	AG			**AB**		
μ	0.002	0.039	0.121	0.001	0.014	0.049
σ	0.000	0.008	0.034	0.000	0.003	0.013
Maximum	0.004	0.056	0.206	0.001	0.022	0.088
Minimum	0.001	0.016	0.046	0.000	0.007	0.016
	ABG			**ABCG**		
μ	0.001	0.020	0.091	0.001	0.020	0.079
σ	0.000	0.004	0.030	0.000	0.006	0.036
Maximum	0.003	0.027	0.171	0.001	0.042	0.214
Minimum	0.001	0.011	0.026	0.000	0.007	0.020

Table 6. Faults applied to 50% of line section length considering two generators

Error (m)	5 Ω	25 Ω	50 Ω	5 Ω	25 Ω	50 Ω
	AG			**AB**		
μ	0.002	0.039	0.121	0.001	0.014	0.049
σ	0.000	0.008	0.033	0.000	0.003	0.013
Maximum	0.004	0.056	0.198	0.001	0.022	0.088
Minimum	0.001	0.016	0.046	0.000	0.006	0.016
	ABG			**ABCG**		
μ	0.001	0.020	0.091	0.001	0.020	0.079
σ	0.000	0.004	0.030	0.000	0.006	0.036
Maximum	0.003	0.027	0.171	0.001	0.042	0.214
Minimum	0.001	0.011	0.026	0.000	0.007	0.020

Comparing Tables 5 and 6 with Tables 1 and 2, it is possible to notice an increase in the error, especially for faults with a resistance of 50 Ω, having more significant increase for single-phase faults from average 0.070 m to 0.121 m. However, the biggest error is again found between buses 118 and 119 when a three-phase to ground fault with a resistance of 50 Ω is applied.

Tables 7 and 8 show the error for faults applied to 50% and 75% of the line section, respectively. The mean error, standard deviation, maximum, and minimum values are the same for both tables, being the largest error found of 0.214 m for three-phase to ground faults with a resistance of 50 Ω. However, a fault located at 99% of the line length between buses 87 and 88, with a resistance of 50 Ω, was not found. This is due to the fact that during the global search, in the first interaction, the line length returned by (3) was longer than the length of this section (5 m). Thus, in this case, the local search is not run in this line section.

In general, the insertion of one more SG increased the errors, and the largest one occurred for two-phase to ground faults with a resistance of 50 Ω (0.095 m), when compared to the previous case (one SG).

Table 7. Faults applied to 75% of line section length considering two generators

Error (m)	5 Ω	25 Ω	50 Ω	5 Ω	25 Ω	50 Ω
	AG			**AB**		
μ	0.002	0.039	0.121	0.001	0.014	0.049
σ	0.000	0.008	0.034	0.000	0.003	0.013
Maximum	0.004	0.056	0.198	0.001	0.022	0.088
Minimum	0.001	0.016	0.046	0.000	0.007	0.016
	ABG			**ABCG**		
μ	0.001	0.020	0.091	0.001	0.020	0.079
σ	0.000	0.004	0.030	0.000	0.006	0.036
Maximum	0.003	0.027	0.171	0.001	0.042	0.214
Minimum	0.001	0.010	0.025	0.000	0.007	0.019

Table 8. Faults applied to 99% of line section length considering two generators

Error (m)	5 Ω	25 Ω	50 Ω	5 Ω	25 Ω	50 Ω
	AG			**AB**		
μ	0.002	0.039	0.121	0.001	0.014	0.049
σ	0.000	0.008	0.033	0.000	0.003	0.013
Maximum	0.004	0.056	0.198	0.001	0.022	0.088
Minimum	0.001	0.016	0.046	0.000	0.007	0.016
	ABG			**ABCG**		
μ	0.001	0.020	0.091	0.001	0.020	0.079
σ	0.000	0.004	0.030	0.000	0.006	0.036
Maximum	0.003	0.027	0.171	0.001	0.042	0.214
Minimum	0.001	0.011	0.025	0.000	0.007	0.019

3.3 Three generators in the system

In the latter case, the presence of the three generators on buses 88, 119, and 122 was considered, totaling a power of 2.3 MVA.

Tables 9, 10, 11, and 12 show the errors obtained for faults at 25%, 50%, 75%, and 99% of the line length, respectively. In general, the same value for mean, standard deviation, maximum, and minimum in these tables. Thus, the largest mean error was for single-phase faults with the resistance of 50 Ω (0.184 m). The largest error was obtained for three-phase to ground faults with a resistance of 50 Ω between buses 118 and 119 (0.314 m).

Table 9. Faults applied to 25% of line section length considering three generators

Error (m)	5 Ω	25 Ω	50 Ω	5 Ω	25 Ω	50 Ω
	AG			**AB**		
μ	0.003	0.055	0.184	0.001	0.019	0.068
σ	0.001	0.010	0.045	0.000	0.003	0.017
Maximum	0.004	0.080	0.308	0.003	0.030	0.121
Minimum	0.001	0.026	0.075	0.000	0.010	0.026
	ABG			**ABCG**		
μ	0.002	0.031	0.117	0.001	0.031	0.120
σ	0.001	0.006	0.035	0.000	0.008	0.051
Maximum	0.004	0.047	0.244	0.002	0.059	0.314
Minimum	0.001	0.015	0.043	0.001	0.012	0.032

Comparing the results of the insertion of three SGs with the results with the insertion of two SGs, it is possible to verify again an increase in the errors, especially when there are single-phase faults with a resistance of 50 Ω, in which there was an increase of 0.110 m in the maximum error. Faults with a resistance of 5 Ω, regardless of type, no significant increase in the average error has been observed.

Table 10. Faults applied to 50% of line section length considering three generators

Error (m)	5 Ω	25 Ω	50 Ω	5 Ω	25 Ω	50 Ω
	AG			**AB**		
μ	0.003	0.055	0.184	0.001	0.019	0.068
σ	0.001	0.010	0.046	0.000	0.003	0.017
Maximum	0.004	0.080	0.308	0.003	0.030	0.121
Minimum	0.001	0.026	0.075	0.001	0.010	0.026
	ABG			**ABCG**		
μ	0.002	0.031	0.117	0.001	0.031	0.120
σ	0.001	0.006	0.035	0.000	0.008	0.052
Maximum	0.004	0.047	0.244	0.002	0.059	0.314
Minimum	0.001	0.015	0.043	0.001	0.012	0.032

Table 11. Faults applied to 75% of line section length considering three generators

Error (m)	5 Ω	25 Ω	50 Ω	5 Ω	25 Ω	50 Ω
	AG			**AB**		
μ	0.003	0.055	0.184	0.001	0.019	0.068
σ	0.001	0.010	0.046	0.000	0.003	0.017
Maximum	0.004	0.080	0.308	0.003	0.030	0.121
Minimum	0.002	0.026	0.075	0.000	0.010	0.026
	ABG			**ABCG**		
μ	0.002	0.031	0.118	0.001	0.031	0.120
σ	0.001	0.006	0.035	0.000	0.008	0.052
Maximum	0.004	0.047	0.244	0.002	0.059	0.314
Minimum	0.001	0.015	0.043	0.001	0.012	0.032

Table 12. Faults applied to 99% of line section length considering three generators

Error (m)	5 Ω	25 Ω	50 Ω	5 Ω	25 Ω	50 Ω
	AG			**AB**		
μ	0.003	0.055	0.184	0.001	0.019	0.068
σ	0.001	0.010	0.046	0.000	0.003	0.017
Maximum	0.004	0.080	0.308	0.003	0.030	0.121
Minimum	0.001	0.026	0.075	0.000	0.010	0.026
	ABG			**ABCG**		
μ	0.002	0.031	0.118	0.001	0.031	0.120
σ	0.001	0.006	0.035	0.000	0.008	0.052
Maximum	0.004	0.047	0.244	0.002	0.059	0.314
Minimum	0.001	0.015	0.043	0.001	0.012	0.032

4. CONCLUSION

This paper proposed an enhancement for impedance-based fault location method with the presence of DGs. The technique depends on the electrical parameters of the substation, from the DGs and loads. For the proposed method, a fault classifier is not required.

The number of DGs affects the method, with the increase on the errors specially for faults with a resistance of 50 Ω. However, the results remained good as it presented errors below 1 m, even with the increasing penetration of DGs. Moreover, fault types and fault resistances, for the same case, did not significantly affect the estimation of the fault location.

Future research might consider inaccuracies in measurement information as well as loads and line parameters. Finally, due to the results and the ease of implementation, it resulted in an excellent potential for application to real problems, since low number of interactions has been required (average of 3 iterations).

REFERENCES

Bahmanyar, A. and Jamali, S. (2017). Fault location in active distribution networks using non-synchronized measurements. *International Journal of Electrical Power & Energy Systems*, 93, 451 – 458. doi:https://doi.org/10.1016/j.ijepes.2017.06.018. URL `http://www.sciencedirect.com/science/article/pii/S0142061517302910`.

Dashti, R., Daisy, M., Shaker, H.R., and Tahavori, M. (2018). Impedance-based fault location method for four-wire power distribution networks. *IEEE Access*, 6, 1342–1349. doi:10.1109/ACCESS.2017.2778427.

Farajollahi, M., Fotuhi-Firuzabad, M., and Safdarian, A. (2019). Simultaneous placement of fault indicator and sectionalizing switch in distribution networks. *IEEE Transactions on Smart Grid*, 10(2), 2278–2287. doi:10.1109/TSG.2018.2794994.

Ferreira, G.D., Gazzana, D.S., Bretas, A.S., and Netto, A.S. (2012). A unified impedance-based fault location method for generalized distribution systems. In *2012 IEEE Power and Energy Society General Meeting*, 1–8. doi:10.1109/PESGM.2012.6345512.

Gururajapathy, S., Mokhlis, H., and Illias, H. (2017). Fault location and detection techniques in power distribution systems with distributed generation: A review. *Renewable and Sustainable Energy Reviews*, 74, 949 – 958. doi:10.1016/j.rser.2017.03.021. URL `http://www.sciencedirect.com/science/article/pii/S1364032117303386`.

Jun Zhu, Lubkeman, D.L., and Girgis, A.A. (1997). Automated fault location and diagnosis on electric power distribution feeders. *IEEE Transactions on Power Delivery*, 12(2), 801–809. doi:10.1109/61.584379.

LaPSEE (2019). Test system - 135 bus. URL `https://www.feis.unesp.br/#!/departamentos/engenharia-eletrica/pesquisas-e-projetos/lapsee/downloads/materiais-de-cursos1193/`.

Mora-Flòrez, J., Meléndez, J., and Carrillo-Caicedo, G. (2008). Comparison of impedance based fault location methods for power distribution systems. *Electric Power Systems Research*, 78(4), 657 – 666. doi:10.1016/j.epsr.2007.05.010. URL `http://www.sciencedirect.com/science/article/pii/S037877960700123X`.

Perez, R., Vásquez, C., and Viloria, A. (2019). An intelligent strategy for faults location in distribution networks with distributed generation. *Journal of Intelligent & Fuzzy Systems*, 36, 1–11. doi:10.3233/JIFS-18807.

Salim, R.H., Resener, M., Filomena, A.D., Caino de Oliveira, K.R., and Bretas, A.S. (2009). Extended fault-location formulation for power distribution systems. *IEEE Transactions on Power Delivery*, 24(2), 508–516. doi:10.1109/TPWRD.2008.2002977.

Sau, R.F., Dardengo, V.P., and de Almeida, M.C. (2020). Allocation of fault indicators in distribution feeders containing distributed generation. *Electric Power Systems Research*, 179, 106060. doi:https://doi.org/10.1016/j.epsr.2019.106060. URL `http://www.sciencedirect.com/science/article/pii/S0378779619303797`.